Project: CREB signaling pathway: PDE4

Probe:

3-(2,5-dimethoxyphenyl)-6-(3,4-dimethoxyphenyl)-7H-[1,2,4]triazolo[3,4-b][1,3,4]thiadiazine

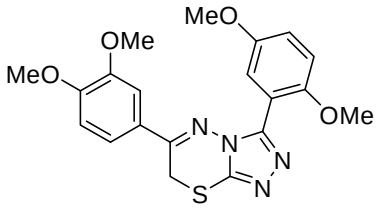

SID: 29217043
Internal IDs: NCGC00165289

PubChem Bioassay Summary Identifier (AID): 662

SID	IC50 (μM)	Antitarget	Selectivity**
29217043	0.013 (PDE4A1A)*	Selected PDE isoforms*, e.g. PDE3B	55.8 (vs PDE3B)

*see table 1; **Selectivity = antitarget IC50/target IC50

Assigned Assay Grant #: MH079867-01

Screening Center Name: NIH Chemical Genomics Center
Principal Investigator of Screening Center: Christopher Austin

Assay Submitter & Institution: Marshall Nirenberg, National Heart Lung & Blood Institute, NIH

Assay or Pathway Target: The cyclic AMP response element-binding proteins

---

Assay provider / Target information

Specific Aim: The cyclic response element-binding proteins (CREB) are a class of transcription factors that bind to selected cAMP response element (CRE) segments of DNA and catalyze the transcription of these genetic sequences.[1] CREB has been implicated as an important regulator of long term memory, and pharmacological enhancement of the CREB signaling pathway in memory may provide an attractive strategy for development of memory enhancing drugs.[2] As the name implies, the primary secondary messenger for initiation of CREB signaling is cAMP. cAMP mediates the actions of numerous protein kinases and is a key element in the regulation of cellular calcium transport. The control of intracellular cAMP and cGMP levels exists as a balance between cAMP and cGMP synthesis via the action of adenylyl cyclase (AC) and guanylyl cyclase, respectively, and degradation

(hydrolysis) by phosphodiesterases (PDEs). The presence of these cyclic nucleotides has regulatory effects on protein kinase A (PKA) and protein kinase G (PKG), the guanine-nucleotide exchange factors (GEFs), and the cyclic-nucleotide gated (CNG) sodium and calcium channels. Small molecules modulators of PDEs (specifically PDE4) are likely to be strong regulators of CREB signaling.

Significance: Abnormalities in the functioning of CREB signaling have been linked to the development and progression of Huntington 's disease and Tubinstein-Taybi syndrome. These abnormalities have been linked to several cancers, in addition to their well-characterized role in the activation of neurons during learning, with changes in gene expression required for long-term memory formation.

Rationale: The rationale for studying this system relies on the discovery of small molecule activators and inhibitors of this signaling pathway, to be used as tools to further characterize the precise roles of CRE up-regulation and down-regulation. In an effort to comprehensively explore the entire signal transduction pathway, a cell-based screen was established, optimized and completed. Using a beta-lactamase reporter-gene under control of the cAMP responsive element, a cell-based assay [CellSensor(TM) CRE-bla CHO developed by Invitrogen Corp.][3] was used to measure forskolin-induced signaling. Library compounds were measured for their ability to potentiate the action of EC_{10} NKH 477, a water soluble forskolin analog, on reporter gene activity. Compounds were screened in a titration series in 1536-well format. Positive and negative modulators were identified based on the AC50 values derived from the screening data.

Screening center information

Assay Implementation and Screening

PubChem Bioassay Name: Cell signaling CRE-BLA (Fsk stim)

List of PubChem bioassay identifiers generated for this screening project (AIDs):

AID	Target	Concentration	Bioassay type
662	CREB Pathway	40 µM – 2.4 nM	Primary qHTS
916	CREB Pathway	40 µM – 4.6 pM	CRE-BLA (Fsk stim) confirmation
907	CREB Pathway	40 µM – 4.6 pM	HEK293 CREB Luciferase confirmation
905	N/A	40 µM – 4.6 pM	CRE-BLA CHO cell cytotoxicity (24 hr)
906	N/A	40 µM – 4.6 pM	CRE-BLA CHO cell cytotoxicity (40 hr)

Primary Assay Description as defined in PubChem:

2000 cells/5uL in Opti-MEM medium containing 0.5% dialyzed FBS, 0.1 mM NEAA, 1 mM sodium pyruvate and 10 mM HEPES was dispensed into 1536-well plates and cells were cultured at 37 degrees Celsius overnight. The next day, 23 nL of compounds or DMSO were delivered to each well using a pin tool, and 1uL of EC10 level of NKH 477, or EC100 level of IBMX, a PDE inhibitor, in the present of NKH 477, or assay medium was added. And then the plates were incubated at 37 degrees Celsius for 3 hours. 1 uL of CCF4-dye mixture was added to each well. After being incubated at room temperature for 2 hours, the plates were measured on an EnVision plate reader at Excitation 405nm, Emission1=460nm and Emission 2=530nm. The %Activity was determined from the ratio of 460nm/530nm.

Table 1. qHTS protocol for CRE-*bla* assay and CRE qHTS Performance Summary

CRE signaling pathway β-lactamase reporter gene assay protocol			
Step	**Parameter**	**Value**	**Description**
1	Reagent	5 uL	2,000 CRE-bla cells
2	Incubation	overnight	Cells adhere and acclimate
3	Library compound	23 nL	38 uM to 0.5 nM titration series
4	Control compound	23 nL	2 nM to 67 uM titration series (IBMX)
5	Reagent	1 uL	Buffer ± potentiator
6	Incubation	3 hrs	Induce CRE reporter
7	Reagent	1 uL	β-lactamase detection solution
8	Incubation	2.5 hrs	CCF4 uptake, de-esterification and processing
9	Detector	Ex 405/8 nm	Perkin Elmer EnVision

Step	Notes
1	Black clear bottom 1536-well plates, single tip dispense of 2000 cells/well into all wells
2	37 °C, 5% CO_2 incubator
3	Pintool transfer of library to columns 5-48
4	Pintool transfer of controls to columns 1-4
5	Single tip dispense for each reagent, Column 1 and 4, subEC_{50} of agonist- 30 nM NKH 477. Column 2 and 3, buffer only
6	37 °C, 5% CO_2 incubator
7	Single tip dispense of 0.6 uM CCF4-AM, 1 mg/ml Pluronic F127 surfactant, 3.5 % PEG 400, 2.6 % TR40, 2 mM probenecid, 0.1 % DMSO
8	Ambient temperature in the dark
9	460/25 nm and 530/20 nm emission filters

Parameter	***Value***
System	Kalypsys robot
Compounds (total # tested)	74,000
Samples (total wells)	755,712
% 6 or 7 pt-titrations	90%
% 14 or 15 pt-titrations	10%
Plates Screened	492
Z'	0.60 +/- 0.11
Signal : Background (S:B)	2.35+/- 0.49

Center Summary of the Primary Screen:
Compounds Screened: 69674, Active: 1744, Inactive: 50125, Inconclusive: 18061

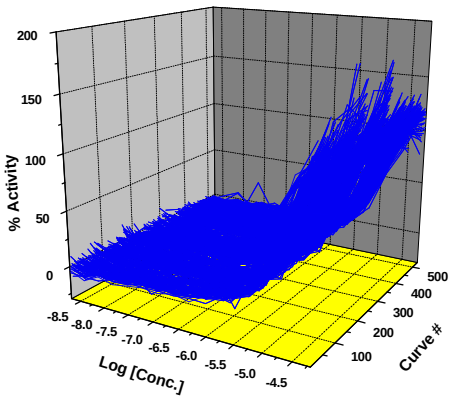

Figure 1a. Intra-plate concentration response titration curves for IBMX in the screening. Each curve was measured in duplicate in column-1 of each assay plate.

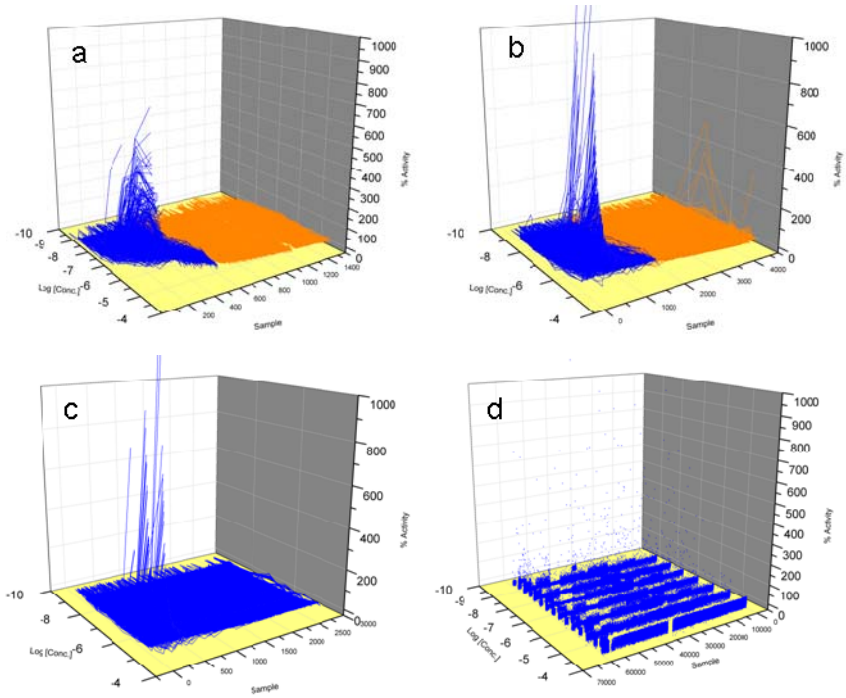

Figure 1b. qHTS curve-fit data from AID 662 binned into curve classifications 1-4 (panels a-d) based classification criteria. Sub-classifications, e.g. 1a vs 1b, are color coded as blue and orange respectively, also see scheme 1 for additional details on qHTS curve classifications.

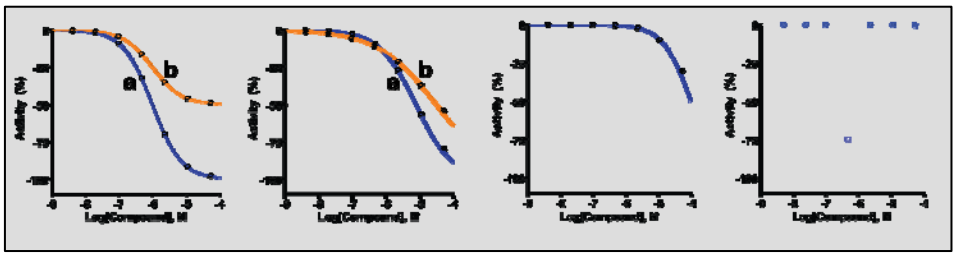

Scheme 1: Example classification scheme for assignment of resulting curve-fit data into classes. Curves fitting the following classification criteria are then used to establish SAR: Class 1 curves display two asymptotes, an inflection point, and r2 ≥0.9; subclasses 1a vs. 1b are differentiated by full (>80%) vs. partial (≤ 80%) response. Class 2 curves display a single left-hand asymptote and inflection point; subclasses 2a and 2b are differentiated by a max response and r2, >80% and >0.9 or <80% and <0.9, respectively. Class 3 curves have a single left-hand asymptote, no inflection point, and a response >3SD the mean activity of the sample field. Class 4 defines those samples showing no activity across the concentration range.

Identification of Active Clusters: Following the qHTS, the concentration response curves (CRCs) data are subjected to a classification scheme to rank the quality of the CRCs as described in Inglese and co-workers[4] (see also scheme 1) Briefly, CRCs are placed into four classes. Class 1 contains complete concentration-response curves showing both upper and lower asymptotes and r^2 values > 0.9. Class 2 contains incomplete CRCs lacking the lower asymptote and shows r^2 values greater than 0.9. Class 3 curves are of the lowest confidence because they are defined by a single concentration point where the minimal acceptable activity is set at 3 SD of the mean activity calculated as described above. Finally, class 4 contains compounds that do not show any CRCs and are therefore classified as inactive. Once an active set of compounds was identified, hierarchical agglomerative clustering with a 0.7 Tanimoto cutoff was performed by using Leadscope (Leadscope Inc., Columbus, OH) fingerprints. For each cluster, maximal common substructures (MCS) were extracted, a manual step of MCS trimming was performed to create a list of scaffolds, and any overlapping scaffolds were abridged to a canonical set. Each scaffold was then represented as a precise definition to indicate descriptors such as the number of attachment points or the ring size variability. All filters were then relaxed to include the entire negative (class 4) assay data.

Target Deconvolution: As the screening paradigm involved a cell based protocol, it was necessary to analyze the active compounds versus selected targets that comprise the CREB signal transduction pathway. As such, we performed secondary assays on selected targets known to modify the CREB signaling pathway. These included assays of Adenylyl cyclase activity, Phosphodiesterase (PDE) activity, Protein Kinase A activity and both luciferase and b-Lacatamase counterscreens.

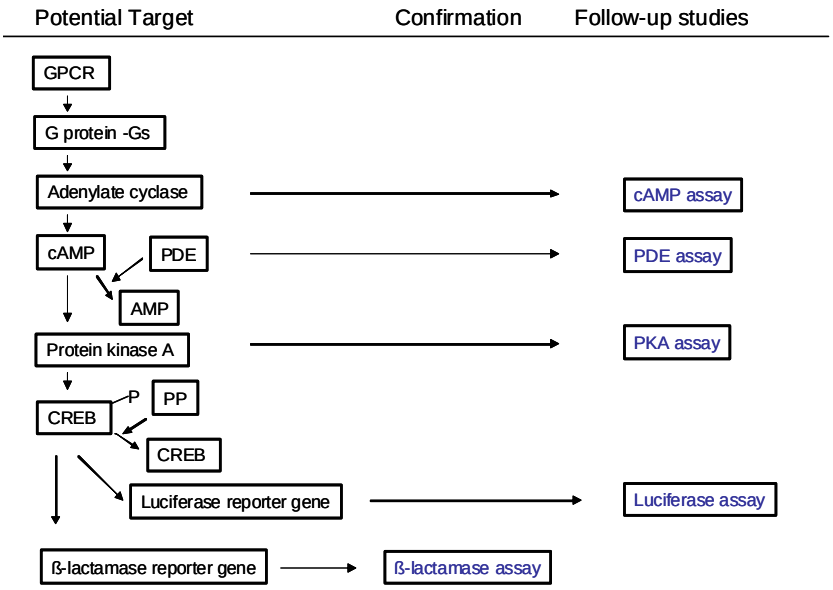

Figure 1. Targets of the CREB signaling pathway.

Lead Identification and Optimization

PDE Background: One of the more impressive lead structures from the standpoint of potency, efficacy, SAR and optimization potential was a series of 3,6-diphenyl-7H-

[1,2,4]triazolo[3,4-b][1,3,4]thiadiazines that were noted to be potent inhibitors of PDE4A during the deconvolution efforts. Modulation of PDE4 regulates numerous phenotypes, including suppression of the inflammatory response, and negative regulation of distressed cells.[3] In particular, the role of PDE4 within the inflammatory responses associated with asthma and chronic obstructive pulmonary disease (COPD) has been widely studied.[5] Memory enhancement and depression indications through PDE4 modulation have additionally been pursued.[6] Further, PDE4 inhibition has recently been studied as a therapeutic intervention within inflammatory bowel disease.[6]

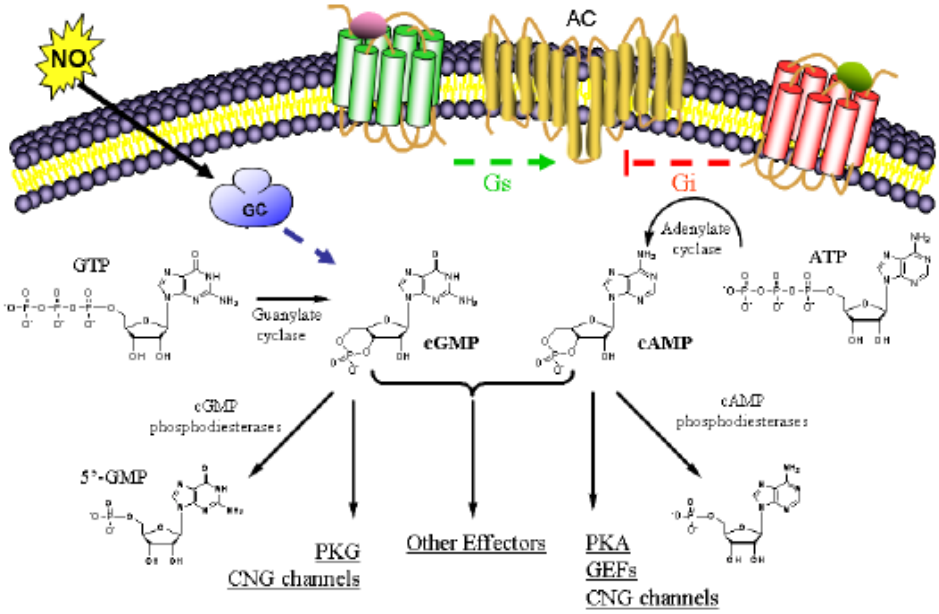

Figure 2. Cartoon description of Cyclic Nucleotide Regulation and Effect by PDE4.

Probe Characterization

Prior Art for PDE4: The PDE class of enzymes contains 11 principal isozymes with 21 characterized gene products. The majority of PDE family members and isoforms have been well-characterized in terms of tissue distribution and substrate affinity. The pharmaceutical sector has focused particular attention on the PDE4 gene family, with inflammation as a primary therapeutic target.[8] As such, numerous small molecules regulate the activity of PDE4 including the ubiquitously utilized rolipram (**1**), and several agents currently being evaluated clinically including roflumilast (**2**), cilomilast (**3**), tofimilast (**4**). The lead structure found in our efforts was the thiadiazine **5A** (Figure 3).

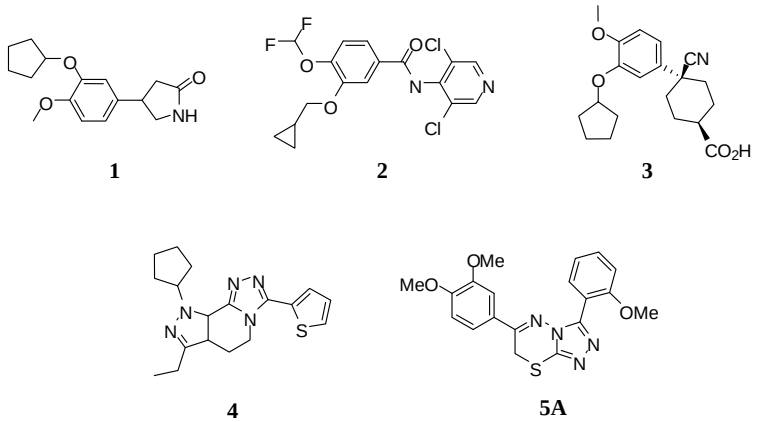

Figure 3. Structures selected PDE4 inhibitors including rolipram (**1**), roflumilast (**2**), cilomilast (**3**), tofimilast (**4**) and 6-(3,4-dimethoxyphenyl)-3-(2-methoxyphenyl)-7H-[1,2,4]triazolo[3,4-b][1,3,4]thiadiazine **5A**.

Synthetic preparation of 5A and selected analogues: In order to expand upon this discovery, novel analogues were prepared via the synthesis of the central heterocycle that was developed based upon existing literature precedence (Scheme 1). Briefly, substituted benzoic acid analogues were transformed to methyl esters and hydrazine in refluxing ethanol provided the needed benzohydrazides. Potassium hydroxide followed by treatment with carbon disulfide produced the carbodithioates and refluxing with hydrazine monohydrate followed by acidification provided the substituted 4-amino-3-phenyl-1H-1,2,4-triazole-5(4H)-thiones in good yields. Concomitantly, several substituted acetophenones were treated with molecular bromine in chloroform to yield the associated α–bromoketones in good yields. A condensation between the substituted 4-amino-3-phenyl-1H-1,2,4-triazole-5(4H)-thiones and substituted α–bromoketones effected by heating an ethanolic solution to elevated temperatures provided the substituted 3,6-diphenyl-7H-[1,2,4]triazolo[3,4-b][1,3,4]thiadiazines. Mass directed preparative LC purification afforded pure samples in good to modest yields. All samples were characterized via proton NMR and HRMS and analytical LC traces of standard 10 mM DMSO solutions confirmed that each product was >90% pure.

Scheme 1

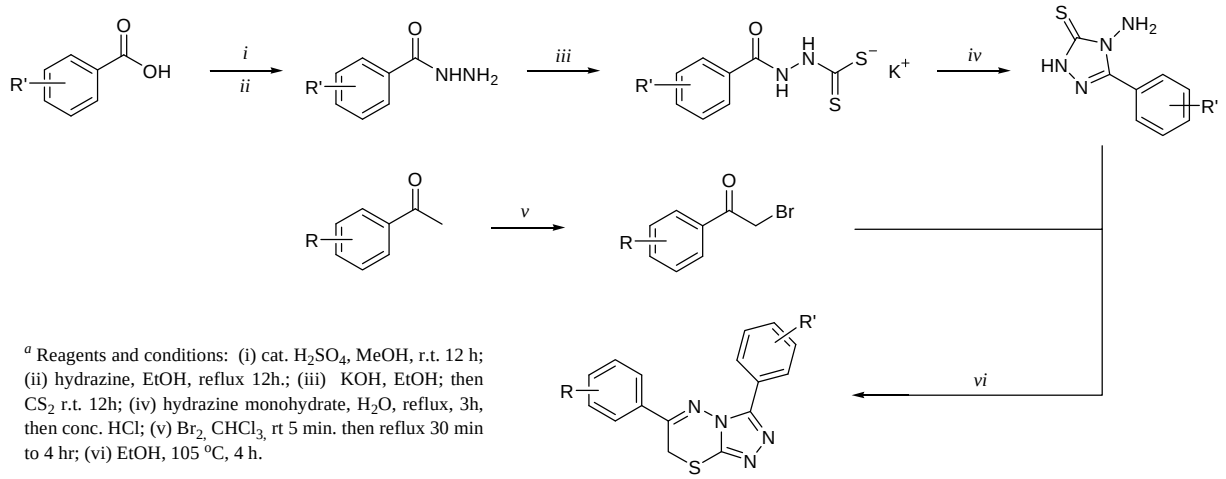

[a] Reagents and conditions: (i) cat. H_2SO_4, MeOH, r.t. 12 h; (ii) hydrazine, EtOH, reflux 12h.; (iii) KOH, EtOH; then CS_2 r.t. 12h; (iv) hydrazine monohydrate, H_2O, reflux, 3h, then conc. HCl; (v) Br_2, $CHCl_3$, rt 5 min. then reflux 30 min to 4 hr; (vi) EtOH, 105 °C, 4 h.

Optimization Strategy: The primary leads were noted to have numerous methoxy substitutions on the adjunct 3- and 6- phenyl rings. Thus, our first exploration of structure activity relationships focused primarily on varied methoxy substitutions on these key

moieties (compounds **5A**-**K**, **6A**-**K**, **7A**-**K**, **8A**-**K**, **9A**-**K**, **10A**-**K** and **11A**-**K** shown in Figure 3). These derivatives were assayed against purified human PDE4A using IMAP technology (Molecular Devices, CA; see appendix for protocol). The inhibitory effects (IC_{50} values) of these compounds are shown in Figure 3.

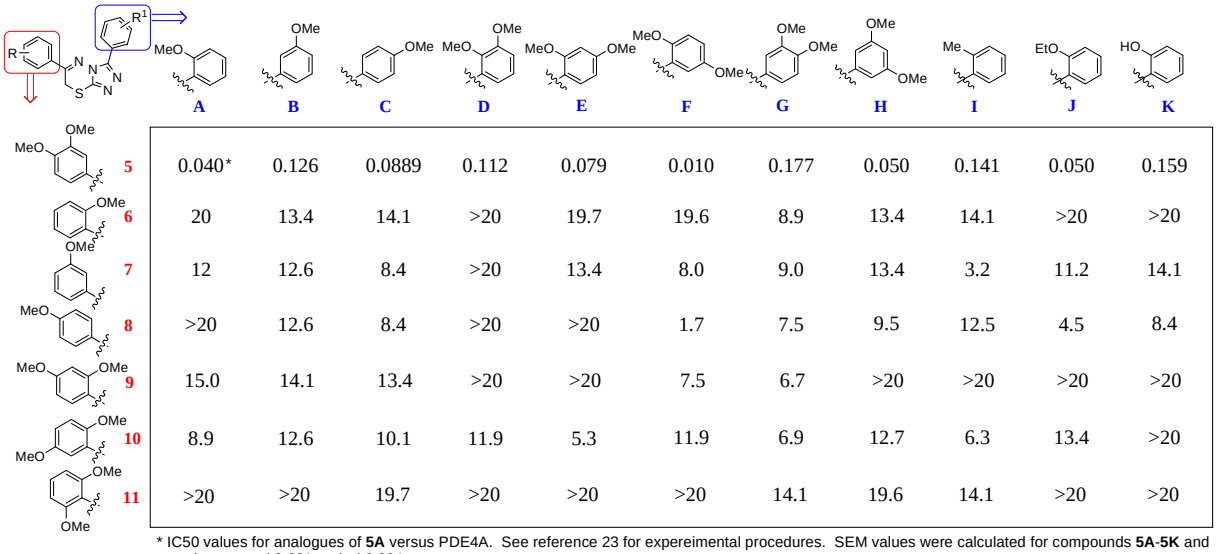

	A	B	C	D	E	F	G	H	I	J	K
5	0.040*	0.126	0.0889	0.112	0.079	0.010	0.177	0.050	0.141	0.050	0.159
6	20	13.4	14.1	>20	19.7	19.6	8.9	13.4	14.1	>20	>20
7	12	12.6	8.4	>20	13.4	8.0	9.0	13.4	3.2	11.2	14.1
8	>20	12.6	8.4	>20	>20	1.7	7.5	9.5	12.5	4.5	8.4
9	15.0	14.1	13.4	>20	>20	7.5	6.7	>20	>20	>20	>20
10	8.9	12.6	10.1	11.9	5.3	11.9	6.9	12.7	6.3	13.4	>20
11	>20	>20	19.7	>20	>20	>20	14.1	19.6	14.1	>20	>20

* IC50 values for analogues of **5A** versus PDE4A. See reference 23 for expereimental procedures. SEM values were calculated for compounds **5A**-**5K** and were between +/-0.001 and +/-0.004.

Figure 4. Schematic representation of substituted 3,6-diphenyl-7H-[1,2,4]triazolo[3,4-b][1,3,4]thiadiazines **5A**-**K**, **6A**-**K**, **7A**-**K**, **8A**-**K**, **9A**-**K**, **10A**-**K** and **11A**-**K** and each compound's apparent IC50 value versus PDE4A.

SAR Evaluation: From this modest library, it was obvious that the 3,4-dimethoxy phenyl substitution on the 5 position of the 3,6-dihydro-2H-1,3,4-thiadiazine ring is a critical functionality for potent PDE4 inhibition (compounds **5A**-**5K**). All derivatives with this functionality had IC_{50} values in the low nanomolar range with the most potent being 3-(2,5-dimethoxyphenyl)-6-(3,4-dimethoxyphenyl)-7H-[1,2,4]triazolo[3,4-b][1,3,4]thiadiazine (**5F**). The phenyl ring attached at the 3 position of the 1,2,4-triazole portion was seemingly less involved in defining the pharmacophore of this structure, as numerous methoxy substitutions had less obvious effects in terms of structure activity relationships. Interestingly, the 3,4-alkoxy moiety (or more appropriately the 3,4-catechol diether) plays a key role in numerous PDE4 inhibitors [as illustrated by the structures of rolipram (**1**), roflumilast (**2**) and cilomilast (**3**) (Figure 3)].[7] Crystallographic analyses of several known inhibitors that share this feature show that a common hydrogen bond between this key functionality and a conserved glutamine residue provides the structural basis for inhibition. Importantly, this glutamine residue (Gln442 in PDEB and Gln369 in PDE4D) is within close proximity to the coordinated Zn^{2+} and Mg^{2+} ions that form the basis for the mechanism of cAMP hydrolysis by PDE4. Given the strong ability of 3,4-dimethoxy derivatives **5A**-**5K** to inhibit PDE4, we surmise that this novel chemotype is inhibiting PDE4 via interaction at the same binding site. Interestingly, the similar 3,4-dimethoxy substitution pattern engineered upon the phenyl ring attached at the 3 position of the 1,2,4-triazole did not convey favorable affects on PDE4 inhibition, as illustrated by compounds **6G**, **7G**, **8G**, **9G**, **10G** and **11G**. This suggests that the interaction between the 3,4 dimethoxy phenyl moiety attached at the 5 position of the 3,6-dihydro-2H-1,3,4-thiadiazine ring places the remainder of the molecule (i.e. the 1,2,4-triazole and the variously substituted phenyl ring attached at the 3 position) in an orientation that interrupts the binding of cAMP and subsequent hydrolysis.

These SAR studies lead to the ultimate realization of compound **5F** as the most potent inhibitor of PDE4A from this series.

Table 2. PDE isoform selectivity data for NCGC00165289

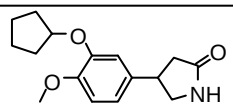

1 (rolipram)

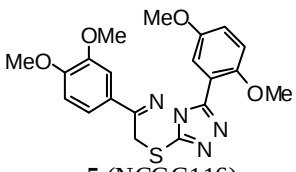

5 (NCGC116)

*PDE isoform**	**1** *IC_{50}/% inh.*	NCGC00165289 *IC_{50}/% inh.*
PDE1A	inactive	inactive
PDE1B	inactive	inactive
PDE1C	inactive	26%
PDE2A	inactive	41%
PDE3A	inactive	1.7 µM
PDE3B	inactive	720 nM
PDE4A1A	102 nM	12.9 nM
PDE4B1	901 nM	48.2 nM
PDE4B2	534 nM	37.2 nM
PDE4C1	40%	452 nM
PDE4D2	403 nM	49.2 nM
PDE5A1	inactive	60%
PDE7A	inactive	73%
PDE7B	inactive	33%
PDE8A1	inactive	57%
PDE9A2	inactive	inactive
PDE10A1	inactive	823 nM
PDE11A4	inactive	inactive

* data generated by BPS Biosciences (CA) [http://www.bpsbioscience.com]and represents either the IC50 value or the % inhibition at 10 uM of compound.

*Selectivity form **5A** against a panel of PDE isoforms:* Having defined this novel chemotype as capable of potent PDE4 inhibition, we next ascertained the selectivity of these compounds against other PDE enzymes [Note: 5A was used for this study prior to the full characterization of **5F**]. IC_{50}'s of **5A** and rolipram (**1**) were determined in biochemical assays for 12 PDE isoforms; results are shown in Table 1. Our lead compound **5A** demonstrated nanomolar inhibitory potency against all three PDE4 isozymes (PDE4A, PDE4B and PDE4D) but ≥100-fold lower potency against the other the nine PDEs tested, including no activity against PDE7A and PDE7B, which are closely homologous to PDE4. Importantly, **5A** showed potent inhibition of the therapeutically important PDE4B isoform, compared to the relatively low potency of rolipram at PDE4B.

Known probe properties:

Center summary of probe properties (solubility, absorbance/fluorescence, reactivity, toxicity, etc.) and recommendations for the scientific use of probe as research tool:

Molecular Weight	412.4622 [g/mol]
Molecular Formula	$C_{20}H_{20}N_4O_4S$
XLogP	3.8
H-Bond Donor	0
H-Bond Acceptor	8
Rotatable Bond Count	6
Tautomer Count	2
Exact Mass	412.120526
MonoIsotopic Mass	412.120526
Topological Polar Surface Area	80

Heavy Atom Count	29
Formal Charge	0
Complexity	583
Isotope Atom Count	0
Defined Atom StereoCenter Count	0
Undefined Atom StereoCenter Count	0
Defined Bond StereoCenter Count	0
Undefined Bond StereoCenter Count	0
Covalently-Bonded Unit Count	1

Appendices:

PDE assay: Inhibition of PDE4A was performed using IMAP technology (Molecular Devices, CA). Briefly, two µl/well of PDE4A1A (BPS Bioscience, CA) mixture (0.05ng/µl PDE4A1A, 10 mM Tris pH 7.2, 0.1% BSA, 10 mM $MgCl_2$, 1 mM DTT, and 0.05% NaN_3, final concentration) was dispensed into 1536-well black/solid bottom assay plates (Greiner Bio-One North America, NC) using a Flying Reagent Dispenser (Aurora Discovery, CA). The plates were centrifuged at 1000 rpm for 30s and then 23 nL compound was transferred to the assay plate using a Kalypsys pin tool. After incubation at room temperature for 5 min, 2 µL/well of cAMP (100 nM, final concentration) was dispensed for a final assay volume of 4 µL /well. The plates were centrifuged at 1000 rpm for 30s, incubated for 40 min at room temperature, and then 4 µL of IMAP binding reagent were added to the assay plate. After 1 to 4 hr incubation at room temperature, the fluorescence polarization (FP) signal (Ex= 485 nm, Em= 530 nm) was measured on Viewlux plate reader (Perkin Elmer, MA).

Representative active and inactive analogs from the qHTS

Structure	NCGC ID Supplier ID PubChem SID	qHTS AC50 (µM)	Follow Up AC50 (µM) (PDE4)	MW	Purity (%)	cLogP (calculated)	Follow Up Curve (PDE4)
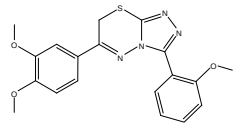	NCGC00071837-01 InterBioScreen: STOCK4S-18669 861731	1.26	0.03	382.4	100	3.33	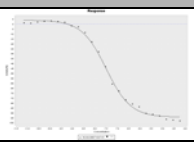
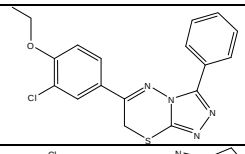	NCGC00052168-01 Chem Div: K243-0178 4240602	0.08	1.26	370.9	100	4.36	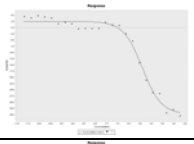
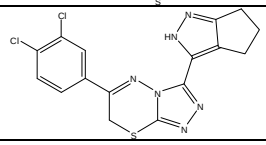	NCGC00070065-01 InterBioScreen: STOCK5S-25894 864669	1.00	7.94	391.3	100	3.82	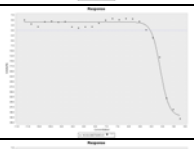
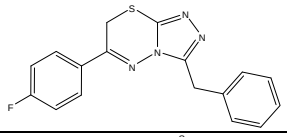	NCGC00038506-01 Enamine: T0502-5295 3717230	>100	12.59	324.4	100	3.37	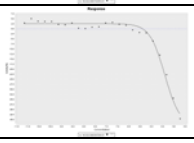
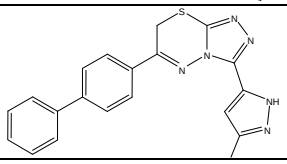	NCGC00068557-01 InterBioScreen: STOCK5S-10193 864226	>100	25.12	372.4	100	4	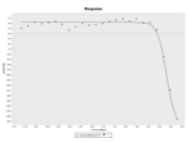

Bibliography:

(1) Carlezon, W.A., Jr. et al. (2005) The many faces of CREB. Trends Neurosci 28 (8), 436-445.

(2) Josselyn, S.A. and Nguyen, P.V. (2005) CREB, synapses and memory disorders: past progress and future challenges. Curr Drug Targets CNS Neurol Disord 4 (5), 481-497.

(3) Huang, Z. et al. (2001) The next generation of PDE4 inhibitors. Curr Opin Chem Biol 5 (4), 432-438

(4) Inglese, J. *et al.* Quantitative high-throughput screening: A titration-based approach that efficiently identifies biological activities in large chemical libraries. *Proc Natl Acad Sci U S A* **103**, 11473-11478 (2006).

(5) Schmidt, D.T. et al. (2000) The effect of selective and non-selective phosphodiesterase inhibitors on allergen- and leukotriene C(4)-induced contractions in passively sensitized human airways. Br J Pharmacol 131 (8), 1607-1618

(6) Dyke, HJ (2007). Novel 5,6-dihydropyrazolo-[3,4-E][1,4]diazepin-4 (1H)-one derivatives for the treatment of asthma and chronic obstructive pulmonary disease. *Expert Opin. Ther. Patents* (17) 1183-1189.

(7) Keshavarizian, A.; Mutla, E.; Guzman, J. P.; Forsythe, C.; Banan, A (2007). Phosphodiesterase 4 inhibitors and inflammatory bowel disease: emerging therapies in inflammatory bowel disease. Expert Opin Investig Drugs 16 (9), 1489-1506.
(8) Zhang, K. Y., P. N. Ibrahim, S. Gillette, and G. Bollag. 2005. Phosphodiesterase-4 as a potential drug target. *Expert Opin. Ther. Targets.* 9:1283–1305.